Kinetics of Dimerization and Interactions of p13^{suc1} with Cyclin-Dependent Kinases†

May C. Morris, Frédéric Heitz, and Gilles Divita*

Centre de Recherches de Biochimie Macromoleculaire, CNRS, 1919 Route de Mende, 34293 Montpellier Cedex 5, France

Received April 22, 1998; Revised Manuscript Received July 22, 1998

ABSTRACT: The impact of p13^{suc1} on the conformation and regulation of cyclin-dependent kinases (cdks) and cyclins was investigated by spectroscopic and rapid kinetic approaches. In the absence of phosphorylation on cdks, p13^{suc1} formed stable complexes, mainly stabilized by hydrophobic interactions, specifically with cdk2 and cdc2. The presence of cyclin A, associated with cdk2 or cdc2, increased the stability of the interaction between cdk2 and p13^{suc1} by a factor of 2. However, cyclin A did not modify the association rate of p13^{suc1} to cdk2, but the dissociation rate, which was decreased 3-fold. Moreover, binding of p13^{suc1} to cdk2 resulted in a 2-fold decrease in the release of nucleotide from cdk2, indicating that p13^{suc1} induces a marked change in the structure of the nucleotide binding site of cdks. On the basis of the structure of cdk2/CksHs1 complex and on our kinetic results, we propose that the binding of Cks proteins to C-lobe of cdk2 is stabilized by the presence of cyclin A and that it may modify the orientation of the loop carrying residues 14 and 15 and their consequent access for dephosphorylation by cdc25 phosphatases. Finally, we have shown that dimerization of p13^{suc1} in the presence of zinc abolishes its interaction with cdks, which suggests that the binding of p13^{suc1} to cdk2 or cdk2/cyclin A may be regulated by dimerization of p13^{suc1} in vivo.

In higher eukaryotes cell cycle progression is governed by members of the cyclin-dependent kinase family (cdks) and by their regulatory cyclin partners. Formation of cdk/cyclin complexes is regulated both by protein/protein interactions and by reversible phosphorylation. Monomeric cdk subunits do not exhibit protein kinase activity, whereas association with their cyclin partner confers basal kinase activity to the complex and further promotes phosphorylation of the cdk on the conserved threonine 161 residue (position in the sequence of cdk2) by the cdk activating kinase complex (CAK), which finally renders the complex fully active (*1*−*3* and references therein).

The activity of cdk/cyclin complexes is also regulated by small proteins from the CKI familly (*4*) that bind and inactivate cdk/cyclin complexes and by a small protein termed Cks (cyclin-dependent kinase subunit). Cks proteins from different species form a family of conserved, small proteins (9−13 kDa) which are essential for cell cycle progression in vivo (*5*−*10*). *Schizosaccharomyces pombe* p13^{suc1} and *Saccharomyces cerevisiae* Cks1 were first isolated and identified as suppressors of certain temperature-sensitive mutations of cdc2 and CDC28, respectively (*6, 11, 12*). Both *S. pombe* p13^{suc1} and *S. cerevisiae* Cks1 are essential for cell viability and have been shown to interact physically with cdc2 and CDC28, respectively (*12, 13*). Two human Cks homologues, CksHs1 and CksHs2, have been isolated and found to complement Cks1 function in budding yeast mutants (*9*). *S. cerevisiae* Cks1 plays a key role at both the G1/S and the G2/M transitions (*14*). Overexpression of p13^{suc1} in *S. pombe* and its microinjection or that of the *Xenopus* homologue p9 in *Xenopus* oocyte extracts delay mitosis significantly through inhibition of cdc2/cyclin B tyrosine dephosphorylation (*11, 15, 16*). However Cks proteins are not direct inhibitors of cdk kinase activity (*8, 17*). Surprisingly, immunodepletion of *Xenopus* p9 during interphase also abolishes entry into mitosis through a failure of cdc2/cyclin B tyrosine dephosphorylation and activation (*16*). Finally, immunodepletion of *Xenopus* p9 during mitosis prevents exit from mitosis through a defect in protein degradation (*16*). Although the product of the *S. pombe suc1* gene, p13^{suc1}, is essential for regulation of cdc2 and cdk2 in vivo (*5*), it is altogether devoid of catalytic activity; moreover its mechanism of regulation is not clearly defined.

The recent determinations of the X-ray structures of fission yeast p13^{suc1} (*18*−*20*) and of the two human isoforms CksHs1 (*21*) and CksHs2 (*22*) have revealed that these proteins can adopt at least two different conformations: monomeric and dimeric. The central structural feature of Cks proteins is a four β-stranded core flanked by two or three small α-helices. Dimers share a common organization in human and yeast proteins, formed by symmetrical exchanges of the C-terminal β-strand between two monomers in their extended β-hinge conformation (*18, 19, 21*). The key region involved in the formation of dimers is a β-hinge which carries residues "HxPEPH", conserved throughout all the members of the Cks family. Endicott et al. have shown that the formation of p13^{suc1} dimers can be induced in the presence of zinc (*18*). p13^{suc1} can therefore exist in three distinct conformations and assembly states: as a β-hairpin single-domain fold, as a β-interchanged dimer, and as a single-domain-folded dimer mediated by zinc ions.

† This work was supported by the CNRS, by a grant from the Association pour la Recherche Contre le Cancer (ARC Contract 1244), and by a grant from the Ligue Nationale Contre le Cancer.

* To whom correspondence should be addressed. Tel: (33) 04 67 61 33 92. Fax: (33) 04 67 52 15 59. E-mail: gilles@puff.crbm.cnrs-mop.fr.

S0006-2960(98)00913-1 CCC: $15.00
Published on Web 09/16/1998

In the present work, we have combined complementary methods including intrinsic and extrinsic fluorescence, as well as size exclusion HPLC, in steady-state and transient kinetic experiments to investigate both the dimerization process of p13^{suc1} as well as the molecular processes of protein/protein interactions between p13^{suc1}, cdks, and cyclins which are essential for eukaryotic cell cycle progression. Finally the impact of the distinct dimeric conformations of p13^{suc1} on its ability to interact with cdks and with cdk/cyclin complexes was quantified and characterized at the molecular level. Our results on the dimerization of p13^{suc1} mediated by zinc indicate that this process occurs in at least two steps: first the binding of zinc to p13^{suc1}, followed by dimerization of the p13^{suc1}/zinc complex. Our studies on the interactions between p13^{suc1}, cdk2, and a cdk2/cyclin complex reveal that only the monomeric form of p13^{suc1} is able to interact with cdk2 or cdk2/cyclin A.

EXPERIMENTAL PROCEDURES

Materials. TSK-250 and TSK-125 Bio-Sil columns were from Bio-Rad. ADP and ATP were purchased from Boehringer Mannheim. Acrylamide and iodide were obtained from Sigma. Mant derivative nucleotides were synthesized as described by Hiratsuka (*23*) and purified according to John et al. (*24*). The purity and stability of nucleoside and nucleotide analogues were checked by reverse-phase HPLC.

Protein Expression and Purification. Yeast p13^{suc1} was expressed and purified as described by Labbé et al. (*25*). Purification was achieved by gel filtration on a Pharmacia Sepharose 75 column: two peaks were eluted, corresponding to the monomeric and dimeric forms of p13^{suc1}, respectively. The two forms of p13^{suc1} were dialyzed and concentrated in buffer containing 50 mM Tris-HCl, pH 7.5, 50 mM KCl, and 50% glycerol. GST-cdk2, GST-cdk7, and cyclin A were overexpressed in *Escherichia coli* and purified to homogeneity as previously described (*26*−*28*). The GST tag moiety was removed by cleavage with factor Xa or thrombin, and the proteins were further purified by size exclusion chromatography. N-Terminal poly(His)-tagged cyclin H and cdc2 were obtained as soluble proteins by overexpression in *E. coli*, as already described (*29*). All proteins were concentrated in a buffer containing 50% glycerol and stored at −80 °C. Protein concentrations were routinely determined according to Bradford (*30*) with bovine serum albumin as a standard.

Size Exclusion HPLC. Size exclusion chromatographies were performed using either one HPLC column (Biorad), TSK-125 (7.5 × 200 mm), or two columns in series, TSK-250 followed by TSK-125 (7.5 × 200 mm). p13^{suc1}, cyclins, cdks, and cdk/cyclin complexes (0.2−2 μM) were incubated for 15 min at 25 °C, then loaded onto the columns, and eluted with 150 mM potassium phosphate or NaCl (pH: 6.8 or 7.2) at a flow rate of 0.8 mL/min. The columns were calibrated with standard proteins including bovine serum albumin (60 kDa), ovalbumin (43 kDa), chymotrypsin (25 kDa), and ribonuclease (13.7 kDa). This method was used for analytical as well as for preparative experiments. Following size exclusion chromatography, the separated complexes were analyzed by SDS−PAGE (*31*).

Fluorescence Experiments. Fluorescence measurements were performed at 25 °C using a Spex II fluorolog spectrofluorometer, with spectral band-passes of 2 and 8 nm, for excitation and emission, respectively. The intrinsic tryptophan fluorescence of p13^{suc1} (0.1−1.0 μM protein) was measured in a fluorescence containing Tris-HCl, pH 7.5, 50 mM KCl, 5% glycerol, and 2 mM EDTA. Dimerization experiments were performed in the absence of EDTA by adding $ZnCl_2$ to the medium. Proteins were incubated for 30 min in fluorescence buffer before starting the experiments, and all measurements were corrected as already described (*32*). Protein samples were excited at 295 nm, and emission spectra were scanned from 310 to 450 nm.

Quenching experiments with either acrylamide or potassium iodide were performed at 25 °C by sequential addition of aliquots from 6−8 M stock solutions, up to 0.4 M final concentration. The solution of potassium iodide contained 0.1 mM sodium thiosulfate, to prevent formation of I_3^-. Using NaCl, we verified that ionic strengths up to 0.4 M did not significantly modify the fluorescence emission of p13^{suc1}. The correction for the inner filter effect due to acrylamide absorption was calculated according to Calhoun et al. (*33*). All values presented correspond to the means of four separate experiments and were corrected according to dilution and by subtracting the blank buffer. The fluorescence quenching data were analyzed according to the Stern−Volmer equation, which assumes that all quenching is collisional (*34*).

Measurement of the Interaction of p13^{suc1} with cdks and cdk/Cyclin Complexes. The binding of monomeric and dimeric forms of p13^{suc1} to cdks and cdk/cyclin complexes was performed using cdks complexed to mant-ATP, by monitoring the enhancement of the mant group fluorescence at 450 nm upon excitation at 340 nm (*29*). In both cases, mant-ATP/protein complexes were kept at a constant concentration of 0.2 μM and incubated for 15 min in the presence of different p13^{suc1} concentrations before starting the experiment. Fitting of titration curves was accomplished using the Grafit software (Erithacus Software Ltd.) with a quadratic equation (*29*). Competition experiments were performed in the presence of different amounts of zinc, up to 1 mM. For higher concentrations of zinc, protein aggregation and precipitation were noted. The apparent dissociation constants were evaluated with a quadratic equation, and a plot of these apparent affinities versus the concentration of zinc yielded an estimation of the dissociation constant of p13^{suc1} for zinc and cdk2. All the results presented correspond to the average of four separate experiments with a standard deviation lower than 5%. For displacement experiments, cdk2/mant-ATP or cdk2/mant-ADP complexes at a concentration of 0.2 μM were incubated in the presence of a 200-fold excess of ATP or ADP, and increasing concentrations of p13^{suc1} were added. Dissociation of the fluorescently labeled nucleotides was monitored according to the quenching of mant fluorescence at 450 nm upon excitation at 340 nm. Data were fitted as already described (*29*).

Rapid Kinetics. Kinetic experiments were performed at 25 °C on an SF-61 DX2 stopped-flow apparatus (High-Tech Scientific, Salisbury, England). Dimerization of p13^{suc1} induced by zinc was followed by measuring changes of intrinsic Trp fluorescence. Tryptophan groups were excited at 290 nm, and the corresponding emission was detected through a filter with a cutoff at 320 nm. Kinetics of p13^{suc1} binding to cdks and cdk/cyclin complexes were performed

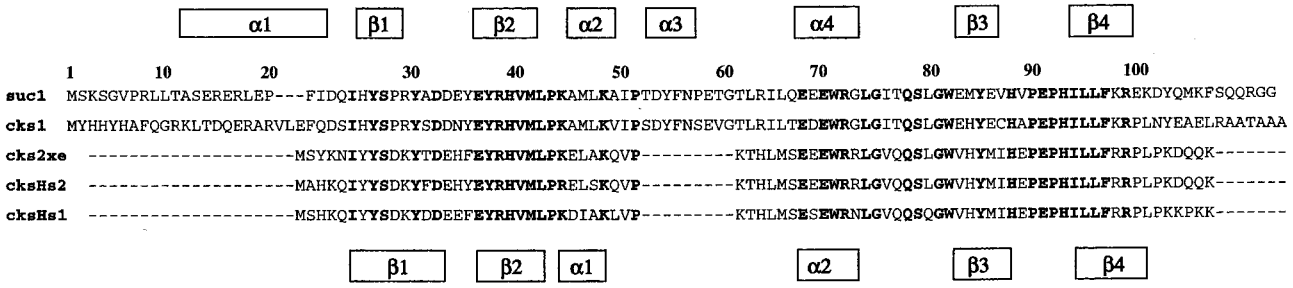

FIGURE 1: Sequence alignement of the different cdk proteins. The sequences of the two yeast homologues *S. pombe* suc1 (*7*) and *S. Cerevisiae* cks1 (*12*) are aligned with those of the two human homologues CksHs1 and CksHs2 (*9*) and the *Xenopus* homologue cks2Xe (*16*). Conserved residues are in bold, and the positions of the structural motifs (α-helices and β-strand) in p13^{suc1} (*18*) and cksHs1 (*21, 22*) crystal structures are shown above and below the sequence alignment, respectively.

by monitoring the fluorescence of mant-ATP through a filter with a cutoff at 408 nm, after excitation at 350 nm. Data collection and primary analysis were performed with the package from High-Tech Scientific, and secondary analysis was performed with the Grafit program (Erithacus, Sofware) using a nonlinear-square procedure to a single or double exponential. Kinetic simulations were performed by using the KinSim program (*35*), and the fitting of the steady-state experiments were performed with the Scientist program (Micromath, UT).

Circular Dichroïsm. Circular dichoism experiments were carried out with a Jobin Yvon mark V spectrometer at 25 °C using quartz cells of various path lengths (from 0.01 to 50 mm) according to the concentration and to the region observed (near or far UV).

RESULTS

Characteristics of the p13^{suc1} Dimer. p13^{suc1} contains two Trp residues which are highly conserved in all Cks proteins, at positions 71 and 82 in its sequence (Figure 1), which confer to the monomeric form of p13^{suc1} an important intrinsic fluorescence with an emission spectrum centered at 344 nm, upon excitation at 295 nm, as already reported (*36*). The dimerization of p13^{suc1} induced in the presence of zinc (*18*) can be monitored by a quenching in its intrinsic fluorescence. Indeed, as shown in Figure 2A, zinc-induced dimerization results in 50% quenching of intrinsic fluorescence with a blue shift of the emission from 344 to 325 nm, which is characteristic of deeply buried Trp residues. In contrast, the β-strand-exchanged p13^{suc1} dimer purified in the absence of zinc presents a fluorescence spectrum centered at 334 nm. Hence, these results suggest that in zinc-induced dimeric forms of p13^{suc1} the environment of the Trp residues is strongly modified compared to that in monomeric or β-strand-exchanged dimeric p13^{suc1}. The differences in intrinsic fluorescence observed offer an interesting potential for investigating the dimerization of p13^{suc1} by both steady-state and rapid kinetics. It should be noted that in the absence of zinc, and in the presence of 2 mM EDTA, no self-association of monomeric p13^{suc1} was observed for a range of protein concentrations from 0.1 to 10 μM.

We have characterized the conformational change of p13^{suc1} upon dimerization by following the accessibility of the Trp residues to two quenchers: acrylamide and iodide. In each case, the Stern−Volmer plots obtained were linear (Figure 2B). K_{sv} constant values of 8.1 and 4.2 M^{-1} were calculated for monomeric p13^{suc1} for acrylamide and iodide,

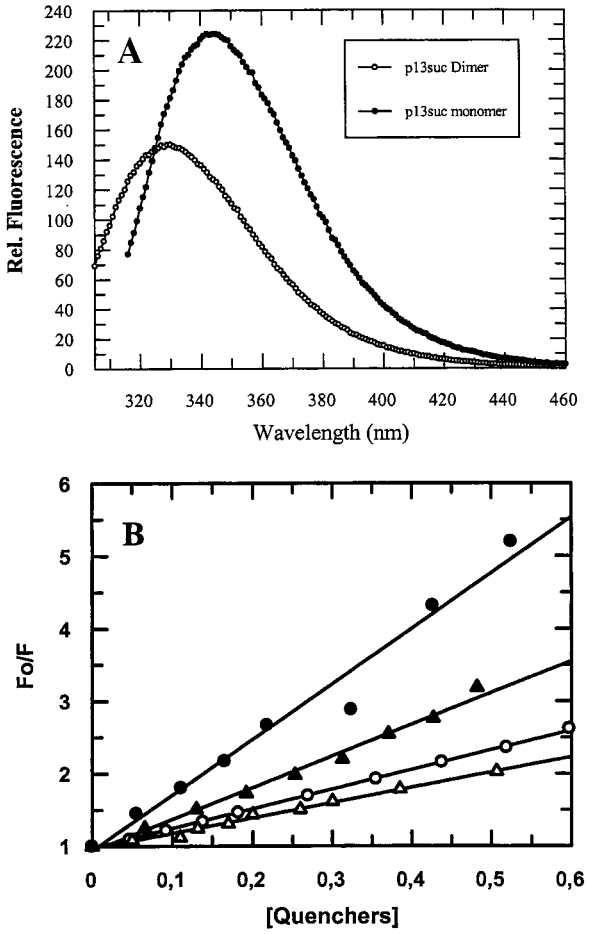

FIGURE 2: Dimerization of p13^{suc1} induced by zinc. A: Fluorescence emission spectrum of monomeric and zinc-induced dimeric p13^{suc1} (2 μM). Monomeric p13^{suc1} was incubated in the absence (●) or presence (○) of equimolar amounts of zinc. Fluorescence emission was measured upon excitation at 295 nm. B: Quenching of fluorescence of monomeric (●,○) and dimeric (▲,△) p13^{suc1} by iodide and acrylamide. The different forms of p13^{suc1} were mixed with increasing amount of acrylamide (closed symbols) and iodide (open symbols). Fluorescence emission was measured at 340 nm upon excitation at 295 nm. Data were analyzed according to Stern−Volmer plots.

respectively. For the zinc-induced p13^{suc1} dimer, the accessibility of the Trp residues toward both quenchers was 3-fold lower, with K_{sv} values of 2.7 and 1.6 M^{-1}, respectively. The decrease in the accessibility of the fluorophores in the β-strand-exchanged dimer was less marked than in the zinc-induced dimer, with K_{sv} values of 3.6 M^{-1} for acrylamide and 2.9 M^{-1} for iodide. Once more, these results reveal

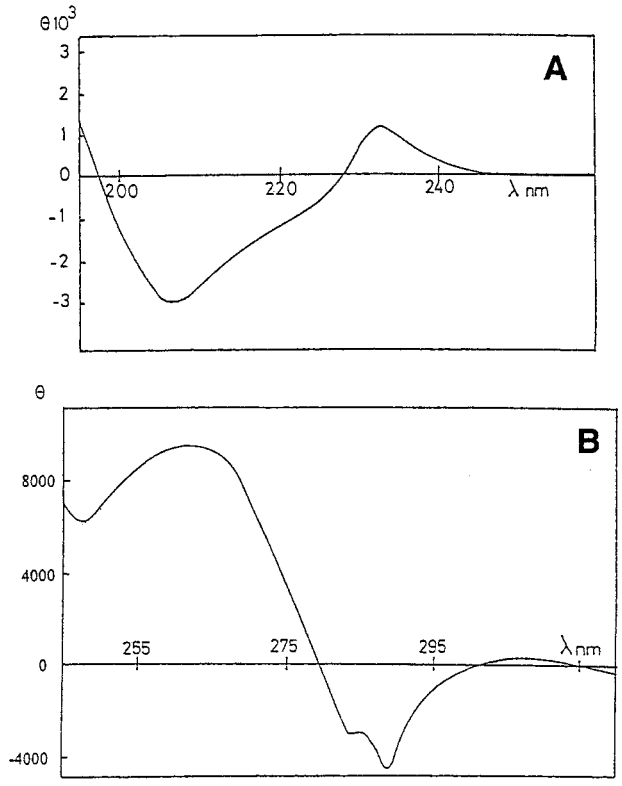

FIGURE 3: CD spectra of p13^{suc1}. The CD spectra of 10 μM p13^{suc1} were recorded in phosphate buffer at pH 7.2. A: Peptide region (θ in deg·cm^2·mol^{-1} in peptide units). B: Aromatic side-chain region (θ in deg·cm^2·mol^{-1} in protein units).

important differences in the accessibility of tryptophan residues in the dimeric versus monomeric forms of p13^{suc1}. Hence, although the secondary structures of both the strand-exchanged and the zinc-induced dimers are similar, the environment of the Trp residues is clearly different.

Secondary Structure of the p13^{suc1} Dimer Monitored by Circular Dichroism. The secondary structures of p13^{suc1} monomer and zinc-induced dimer were investigated by circular dichroism (CD). As shown in Figure 3B, the CD spectrum of monomeric p13^{suc1} presented a very particular feature: a characteristic strong dichroic signal in the side-chain absorption region (290 nm), in perfect agreement with the existence of aromatic clusters. This was further confirmed by analysis of structural features in the far-UV region, which, as shown in Figure 3A, yielded a spectrum characterized by two unusual extrema, the one positive, the other negative, centered at 230 and 208 nm, respectively (*36*). This type of spectrum does not appear to reflect the presence of any known polypeptide conformation or mixture of known conformation. In the absence of disulfide bridges, the band at 230 nm can be attributed to the Trp residues (*37* and references therein), whereas the band at 208 nm can be associated with the presence of α-helices. It should however be noted that in the present case, due to the presence of tyrosine engaged in the aromatic clusters, an aromatic origin of the band at 208 nm cannot be excluded. Measurements in the far-UV region constitute a good means of detecting structural changes which arise upon variations in the medium. This approach was therefore used to check whether the zinc-induced dimerization of p13^{suc1} inferred modifications in its CD spectrum. However, no dramatic change occurred upon binding of zinc, which suggests that the overall conformation

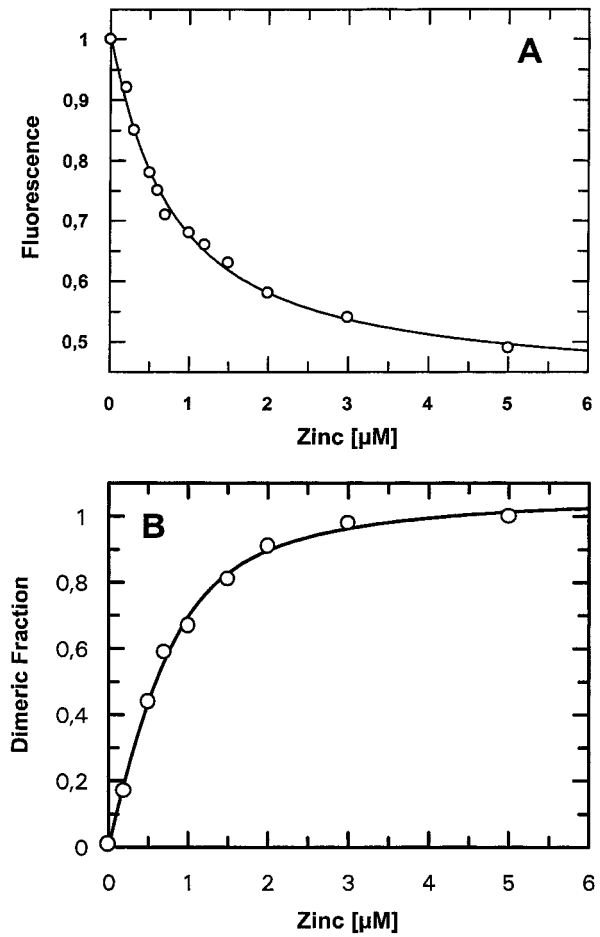

FIGURE 4: Titration of dimerization of p13^{suc1} in the presence of zinc. A: Fluorescence spectroscopy. A fixed concentration of p13^{suc1} (0.2 μM) was titrated with increasing concentrations of $ZnCl_2$. Dimerization of p13^{suc1} was monitored by following the quenching of intrinsic Trp fluorescence at 340 nm, upon excitation at 295 nm. Data were fitted according to the model of a sum of two equilibrium reactions: first zinc binding followed by dimerization, both of which induce quenching of the fluorescence, with the following equation $\Delta F = \Delta F_1[\text{zinc}] + \Delta F_2[\text{p13}^{suc1}/\text{zinc}]$. Intermediate fluorescence values for each concentration of zinc were determined by simulation and fitted as described in Experimental Procedures. B: Size exclusion HPLC. p13^{suc1} (0.2 μM) was incubated with increasing concentrations of $ZnCl_2$ (0−5 μM) and applied onto size exclusion HPLC columns. The dimeric fraction was quantified by size exclusion chromatography.

of monomeric p13^{suc1} is not significantly different from that of the dimer.

Zinc-Induced Dimerization of p13^{suc1}. Using the properties of intrinsic fluorescence of monomeric versus dimeric forms of p13^{suc1}, we investigated the process of p13^{suc1} zinc-induced dimerization. As reported in Figure 4A, the titration curve of p13^{suc1} dimerization obtained by adding increasing concentration of zinc results in a maximal quenching value of 50%. In contrast, no dimerization or self-association of p13^{suc1} was observed in the presence of an excess of Ca^{2+} or Mg^{2+}. The formation of dimeric p13^{suc1} was also investigated by size exclusion chromatography. p13^{suc1} (0.2−2 μM) was applied onto a TSK-125 HPLC column and eluted with 50 mM KH_2PO_4, 150 mM NaCl (pH: 7.2) at a flow rate of 0.8 mL/min. This method was used for the quantification of the ratio of p13^{suc1} dimer in the presence of increasing amounts of zinc. The titration curve obtained by size exclusion chromatography was monophasic (Figure

4B) and revealed that p13^{suc1} was fully dimeric for a concentration of zinc which promotes maximal quenching of fluorescence in Figure 4A (2 μM). This result is in agreement with the value reported from the X-ray structure of the p13^{suc1} dimer (*18*) and confirms the presence of only one zinc binding site per monomer of p13^{suc1}. These results demonstrate that the quenching of intrinsic fluorescence of p13^{suc1} can be directly correlated to the appearance of the dimeric form of the protein.

The quenching of intrinsic fluorescence induced upon binding of zinc to p13^{suc1} was used for monitoring the dimerization kinetics of p13^{suc1}. As shown in Figure 5A, biphasic kinetics were obtained, when the two components p13^{suc1} (0.2 μM) and zinc (3 μM) were mixed in a stopped-flow apparatus. We have interpreted these data with the following hypothetic model, in which the first equilibrium corresponds to the formation of p13^{suc1}/zinc complex and the second to the dimerization of the preformed p13^{suc1}/zinc complex. Both induce quenching of intrinsic fluorescence of p13^{suc1}.

$$\text{zinc} + \text{p13}^{suc1} \underset{k_{-1}}{\overset{k_1}{\leftrightarrow}} \text{p13}^{suc1}/\text{zinc} \quad (1)$$

$$\text{p13}^{suc1}/\text{zinc} + \text{p13}^{suc1}/\text{zinc} \underset{k_{-2}}{\overset{k_2}{\leftrightarrow}} [\text{p13}^{suc1}/\text{zinc}]^2 \quad (2)$$

Figure 5B shows a plot of the pseudo-first-order rate constant for the initial association of zinc with p13^{suc1} (corresponding to the fast phase in the experiment) versus the concentration of zinc which is linear up to a concentration of 7 μM and a rate of 14 s^{-1}. In this experiment the concentration of p13^{suc1} is fixed to 0.2 μM. In contrast, for concentrations of zinc greater than 10 μM, the kinetics could not be analyzed clearly, due to protein oligomerization or precipitation. An association rate constant (k_1) of $2.6 \pm 0.5 \times 10^6$ M^{-1} s^{-1} and a dissociation rate constant (k_{-1}) of 0.8 $^{-1}$ were calculated from the slope and the intercept, respectively. This dissociation rate constant was taken together with the rate constant for the dissociation of the dimeric complex to calculate an equilibrium dissociation constant K_{d1} of 0.4 ± 0.1 μM for the binding of zinc to p13^{suc1}.

In contrast the second part of the kinetics is not dependent on the concentration of zinc. Assuming that this step corresponds to the dimerization of the p13^{suc1}/zinc complex, we performed the same experiment with different concentrations of p13^{suc1} ranging between 0.1 and 1.5 μM and a saturating concentration of zinc (7 μM). The observed association rate constant increased almost linearly with the concentration of p13^{suc1}, with an association rate constant (k_2) of $4.8 \pm 1 \times 10^6$ M^{-1} s^{-1} (Figure 5C) and a very low dissociation rate constant $k_{-2} < 0.005$ s^{-1} estimated by the intercept of the plot. Taken together these two rate constants lead to an equilibrium constant for the dimerization $K_{d2} < 1$ nM.

Accordingly, the quenching of fluorescence of p13^{suc1} upon dimerization induced by zinc, reported in Figure 4A, is in fact the sum of two equilibrium reactions, the first involving binding of zinc, followed by dimerization, both of which induce quenching of the fluorescence with relative amplitudes of 1.2/1. The final titration curves are the result of the sum of two equilibria (eqs 1 and 2), which can be fitted with the following model: $\Delta F = \Delta F_1[\text{zinc}] + \Delta F_2\,[\text{p13}^{suc1}/\text{zinc}]$, where ΔF_1 and ΔF_2 correspond to the quenching of fluorescence due to binding of zinc and to dimerization of p13^{suc1}, respectively. The intermediate fluorescence values for each concentration of zinc were determined by simulation with the KinSim program, using the rate constants obtained from transient kinetics. Best fits were obtained for dissocia-

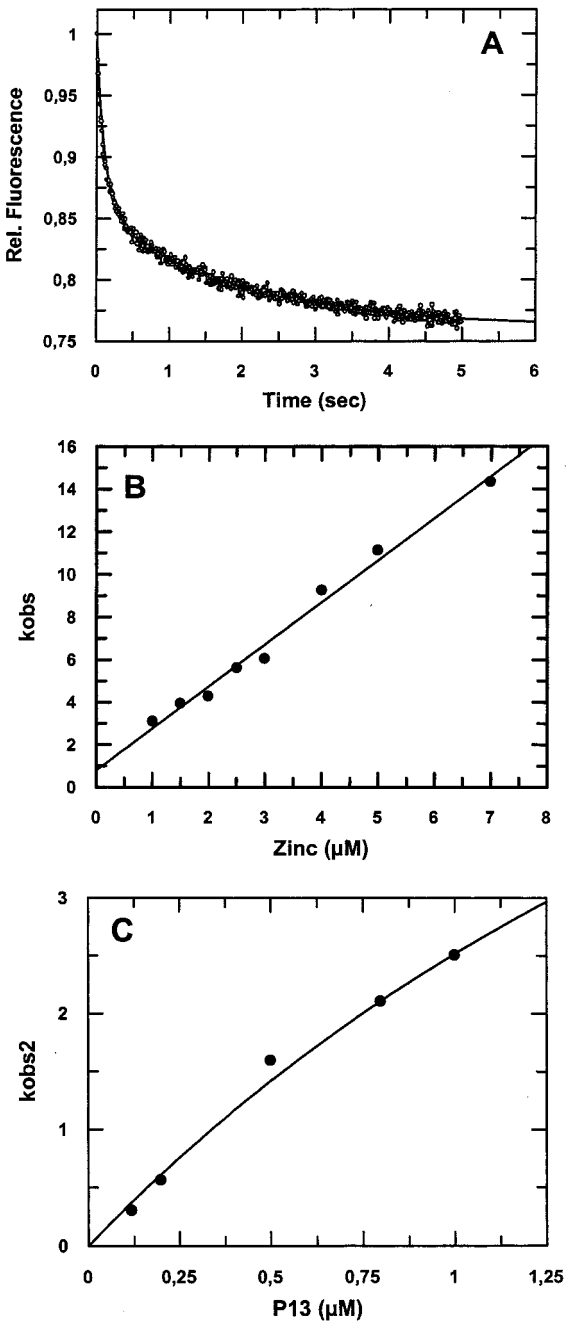

FIGURE 5: Kinetics of dimerization of p13^{suc1}. A: Kinetics of dimerization of p13^{suc1} (0.2 μM) in the presence of 3 μM $ZnCl_2$. Excitation was performed at 290 nm, and fluorescence emission was monitored through a cutoff filter (320 nm). Curves were fitted as a sum of two exponential terms. B: Dependence of the fitted pseudo-first-order rate constant k_{obs} for the initial association of zinc with p13^{suc1} on the zinc concentration. The association and dissociation rate constants were calculated from the slope and the intercept of the linear fit. C: Dependence of the fitted rate constant k_{obs2} for the dimerization of p13^{suc1}/zinc complex on the concentration of p13^{suc1}. The association and dissociation rate constants were estimated from the slope and the intercept of the linear part of the fit.

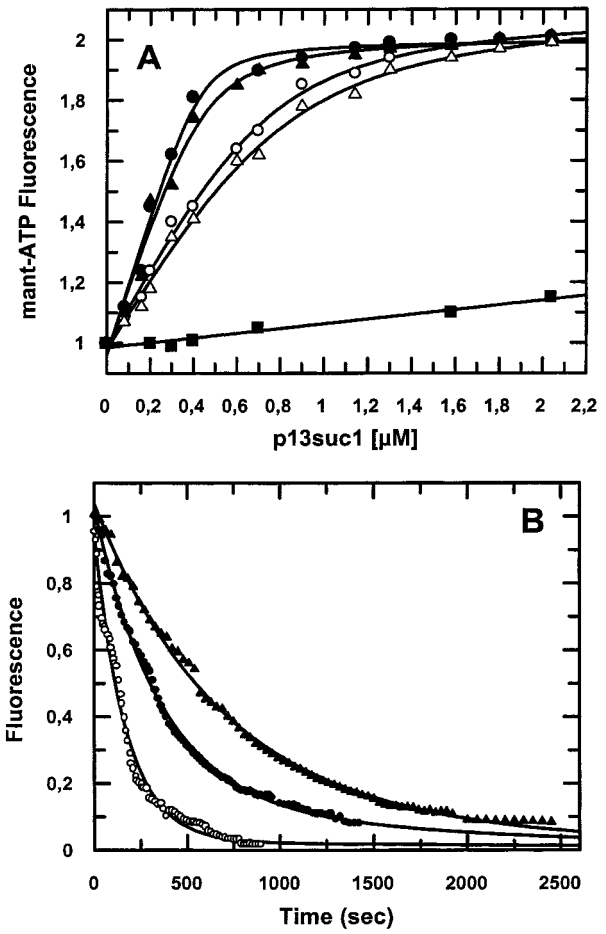

FIGURE 6: Binding titration of p13^{suc1} to cdks and cdk/cyclin complexes. A: Cdk2 (○), cdc2 (△), cdk7 (■) (0.2 μM), and cdk2/cyclin A (●) and cdc2/cyclin A (▲) complexes (0.2 μM) previously saturated with mant-ATP (1 μM) were titrated with increasing concentrations of p13^{suc1}. The enhancement of mant-ATP fluorescence was monitored at 450 nm upon excitation at 340 nm, and the experiments were fitted using a standard quadratic equation. B: Mant-ATP displacement. The mant-ATP release from cdk2 (0.2 μM) by a 200-fold excess of ATP was monitored in the absence (○) and presence of an equimolar concentration of cyclin A (▲) or 3 μM p13^{suc1} (●). The decrease of mant-ATP fluorescence was monitored at 450 nm, and the kinetics were fitted as a single exponential.

tion constants of 1.2 μM and 0.9 nM for zinc and dimerization, respectively (Figure 4A). That these values should be close to those obtained by transient kinetics ($K_{d1} = 0.384$ μM; $K_{d2} = 1.05$ nM) validates our two-equilibria model and thus enables us to propose that dimerization of p13^{suc1} in fact corresponds first to binding of zinc, followed by very tight dimerization.

Binding of p13^{suc1} to cdks and cdk/Cyclin Complexes. The binding of monomeric and dimeric p13^{suc1} to cdks and cdk/cyclin complexes was monitored using cdks, complexed to a mant-ATP group, and by measuring changes in the extrinsic fluorescence of mant-ATP. Indeed, as already reported (*29*), mant-ATP presents high affinity for cdks and constitutes a very sensitive probe for monitoring the interactions between cdks and its partners. Mant-ATP/cdk2, mant-ATP/cdc2, and mant-ATP/cdk7 complexes were formed prior to addition of p13^{suc1} and then titrated with increasing concentrations of p13^{suc1}. As shown in Figure 6A, the binding of monomeric p13^{suc1} to cdk2 or cdc2 and to cdk2/cyclin A or cdc2/cyclin A complexes induced a 2-fold increase in the

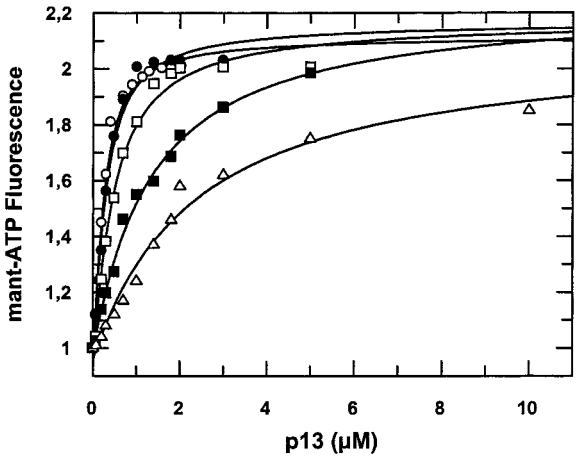

FIGURE 7: Binding titration of p13^{suc1} to cdk2 in the presence of zinc. Cdk2 (0.2 μM) previously saturated with mant-ATP (1 μM) was titrated with increasing concentrations of p13^{suc1} in the absence (○) and presence of zinc 50 μM (●), 200 μM (□), 500 μM (■), and 1 mM (△). The enhancement of mant-ATP fluorescence was monitored at 450 nm upon excitation at 340 nm, and the experiments were fitted as described in Figure 6A.

fluorescence of mant-ATP. All the titration curves obtained were monophasic, with K_d values of 150 and 170 nM for cdk2 and cdc2, respectively, and of 78 and 90 nM for cdk2/cyclin A and cdc2/cyclin A complexes, respectively. In contrast, no binding of p13^{suc1} to cdk7 or cdk7/cyclin H was observed up to a concentration of 10 μM p13^{suc1}. At saturating concentrations of p13^{suc1}, the complexes formed were separated by gel filtration chromatography (data not shown). Both cdk2/p13^{suc1} and cdk2/cyclin A/p13^{suc1} eluted as complexes, which reveals that monomeric p13^{suc1} interacts strongly with cdks and that the presence of cyclin A does not interfere with this interaction. In contrast, no interaction between the two different dimeric forms of p13^{suc1} and cdks or cdk/cyclin complexes was detected, up to a concentration of 10 μM p13$^{suc1.}$

Mant-ATP bound to cdks can be fully displaced by an excess of unlabeled nucleotide, resulting in a 10-fold decrease in the fluorescence of the mant group. As already shown elsewhere (*29*), the dissociation rate of mant-ATP from cdk2 using a 200-fold excess of ATP occurred according to a single exponential with a rate constant of 5.4×10^{-3} s^{-1}. When this experiment was repeated in the presence of saturating concentrations of p13^{suc1}, the dissociation rate constant of mant-ATP from cdk2 was reduced to a value of 2.1×10^{-3} s^{-1} (Figure 6B), which is 2-fold faster compared to the values obtained for a saturating concentration of cyclin A (1.2×10^{-3} s^{-1}). The rate of the displacement kinetics was dependent on the concentration of p13^{suc1}, and a maximal effect was obtained for a concentration of p13^{suc1} of 3 μM, a value close to that obtained with both fluorescence and size exclusion titrations.

The zinc-induced dimeric form of p13^{suc1} does not interact with either cdk2 or the cdk2/cyclin A complex. As such, we were interested in furthering our understanding of the role of zinc in the regulation of the interaction of p13^{suc1} with its partners. With this aim, we performed titrations as described above in the presence of different concentrations of zinc ranging from 10 μM to 1 mM. As shown in Figure 7, in all cases, the fluorescence increased similarly 2.1-fold, whatever the concentration of zinc used. In contrast, the

slope of the titration curve was dependent on the concentration of zinc, due to competition between zinc and cdk2. Each curve was fitted to a quadratic equation yielding an apparent dissociation constant, which was then plotted against the concentration of zinc. This resulted in a straight line, indicating that zinc and cdk2 compete for the same binding domain on p13^{suc1}, in perfect agreement with our observation that dimeric p13^{suc1} did not bind to cdk2. In addition, the displacement of cdk2 by zinc was extremely low, as only 10% of cdk2/p13^{suc1} complexes were displaced with 1 mM zinc (data not shown). These data can be explained by the fact that binding of zinc is the limiting step in the dimerization of p13^{suc1}. Accordingly, the limiting intracellular localized concentration of zinc could explain why dimeric forms of p13^{suc1} have not been found in vivo.

Kinetics of p13^{suc1} Binding to cdks and cdk/Cyclin Complexes. The kinetics of p13^{suc1} binding to cdk2 and the cdk2/cyclin A complex were investigated in a series of stopped-flow experiments. As for the above experiments, cdk2 was complexed to mant-ATP, and association rate constants for the formation of cdk2/p13^{suc1} and cdk2/cyclin A/p13^{suc1} complexes were determined by recording the increase in the fluorescence of mant-ATP after mixing differents concentrations of p13^{suc1} with constant amounts of cdk2/mant-ATP or cdk2/mant-ATP/cyclin A. Figure 8A presents typical kinetics obtained for a concentration of p13^{suc1} of 4 μM. Fitting of the time scale yielded a single exponential term 2-fold faster for the cdk2/cyclin A complex than for monomeric cdk2. In both cases, the association reactions measured under pseudo-first-order conditions yielded a linear relationship between the observed rate constant (k_{obs}) and the concentration of p13^{suc1}. The slope of the linear fit of the observed rate constant versus the concentration of p13^{suc1} yielded a similar association rate constant (k_{on}) for cdk2 and cdk2/cylin A of 2.1×10^7 and 2.8×10^7 M^{-1} s^{-1}, respectively (Figure 8B). In contrast the dissociation rate constant (k_{off}) was 3-fold faster for cdk2 than for cdk2/cyclin A with values of 5.7 and 2.1 s^{-1}, respectively. These results show that although the presence of cyclin complexed to the cdk2 does not significantly modify the binding kinetics of p13^{suc1}, it does decrease the off-rate kinetics of p13^{suc1}. As a consequence, the calculated dissociation constant is 3-fold lower for cdk2/cyclin A (75 $\pm$ 12 nM) or cdc2/cyclin A (82 $\pm$ 21 nM) complexes than for monomeric cdk2 (271 $\pm$ 33 nM) or cdc2 (224 $\pm$ 38 nM).

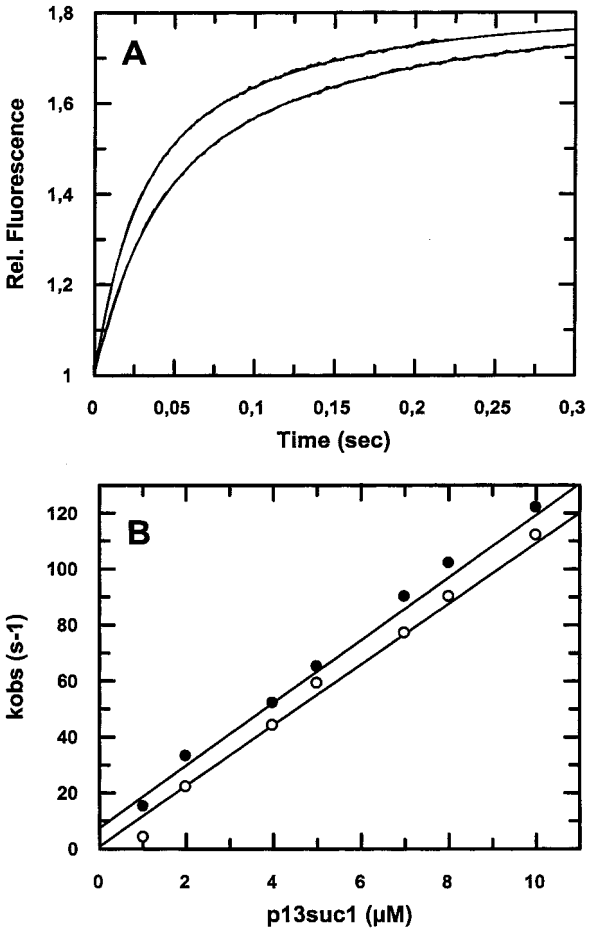

FIGURE 8: Kinetics of binding of p13^{suc1} to cdk2 and cdk2/cyclin A. A: Kinetics of the interaction of p13^{suc1} (4 μM) with cdk2 (0.2 μM) and cdk2/cyclin A (0.2 μM). Excitation was performed at 350 nm, and fluorescence emission of mant-ATP was monitored through a cutoff filter (408 nm). Curves were fitted using a single-exponential term. B: Dependence of the fitted pseudo-first-order rate constant k_{obs} on the concentration of p13^{suc1} in the interaction of p13^{suc1} with cdk2 (○) and cdk2/cyclin A (●). The association and dissociation rate constants were calculated from the slope and the intercept of the linear fit.

DISCUSSION

Cks proteins are small ubiquitous subunits of cyclin-dependent kinases, essential for cell cycle progression in all eukaryotes, which seem to be involved in multiple stages of cdk/cyclin regulation (*5, 10*). Despite their essential nature and apparent multiple functionality, the precise function as well as the regulation of Cks proteins in cell cycle progression still remain elusive. It has however recently been proposed that oligomerization of Cks proteins may be a critical step for their biological function and that multimers of Cks may constitute a negative regulatory state (*10, 21, 22, 38*). In the present work, we have combined biophysical and kinetic approaches to investigate the mechanism of zinc-induced dimerization of p13^{suc1} and the parameters which control its interaction with cdks and cdk/cyclin complexes. On the basis of our kinetic results and taking into account X-ray crystallographic data available, we can now propose a mechanism to explain how the interaction between p13^{suc1} and both cdks and cdk/cyclin complexes occurs and how it may play a role in cell cycle progression.

Zinc-Induced Dimerization of p13^{suc1}. The three forms of recombinant p13^{suc1}: monomeric, the β−strand-exchanged dimer, and the zinc-induced dimer, were overexpressed, purified, and characterized at the molecular level. All Cks proteins contain two highly conserved Trp residues at positions 71 and 82 in p13^{suc1} (Figure 1), which are strategically located in the structure of Cks proteins and constitute good tools for investigating the structure−function relationship of this protein. Trp^{71} is located in α-helix 4 which is involved in stabilizing the phosphate binding domain of CksHs1 (21), and Trp^{82} is located at the base of β-strand 3, which is at the interface close to the zinc binding motif, in the p13^{suc1} β-hairpin dimer (*18*). The corresponding Trp residue (Trp^{54}) in CksHs1 is a key residue in its phosphate analogue binding site and is involved in its interaction with cdk2 (*21, 38*). Moreover, β3- and β4-strands are involved in the β-interchanged dimer of both p13^{suc1} and CksHs1 (*19, 21, 22*).

In the monomeric form of p13^{suc1}, the conserved Trp residues are buried and confer an important intrinsic fluorescence to p13^{suc1} with an emission maximum centered at 344 nm. Zinc-induced dimerization of p13^{suc1} resulted in a large decrease (50%) in its intrinsic fluorescence with a 19-nm blue shift of the maximal emission wavelength, which revealed that the Trp residues became less accessible to the solvent in the dimeric form of p13^{suc1}. These results were indeed confirmed by a 3-fold decrease in their accessibility toward quenchers such as iodide and acrylamide. This is not surprising, considering that Trp^{82} is documented as being located in a positively charged cluster involved in dimer formation (*18*). It should however be noted that, despite this important change in the accessibility of tryptophan groups in the dimeric form of p13^{suc1}, circular dichroism measurements did not reveal significant differences between the secondary structures of the monomer and those of the zinc-induced dimer, as also reported from the crystallographic structure of dimers (*18*−*21*).

In the strand-exchanged p13^{suc1} dimer purified in the absence of zinc, the decrease in solvent accessibility of the Trp residues is less marked than in the zinc-induced dimer, which indicates that, although the secondary structures of both dimers are similar, the environment of their Trp residues is different and can directly be correlated with differences in the molecular surface accessibility between the β-interchanged dimer and the β-hairpin single-domain fold of p13^{suc1}.

Both steady-state and rapid kinetic experiments have shown that p13^{suc1} forms stable dimers in the presence of zinc with high affinity in a nanomolar range. The dimerization of p13^{suc1} constitutes a complex kinetic process, composed of at least two equilibrium reactions (eqs 1 and 2); the first equilibrium corresponds to the binding of one molecule of zinc per molecule of p13^{suc1} with a dissociation constant of 0.4 μM, followed by a very tight [P13^{suc1}/zinc]−[p13^{suc1}/zinc] association, with a dissociation constant of 1 nM. These results indicate that binding of zinc is the limiting step in the formation of the p13^{suc1} dimer, as only p13^{suc1}/zinc complexes are able to form dimers. Given that we did not observe any dimerization or self-association in the presence of cations other than zinc, such as Mg^{2+} or Ca^{2+}, we conclude that zinc is a specific mediator of dimer formation and that such a dimerization may be of biological relevance in vivo. In this respect, it should be reminded that Reed et al. have reported that the kinase activity of *S. cerevisiae* CDC28 is controlled by the presence of zinc (*39*). However, this dimeric form of p13^{suc1} remains specific to yeast Cks proteins, and several groups (*40*, *41*) have clearly observed the lack of dimerization of the human form of CksHs1 in the presence of zinc. This is not surprising given that the major residues involved in the zinc-binding motif (His^{26} and Asp^{23}) are only conserved in yeast Cks proteins (Figure 1).

Mechanism of Formation of p13^{suc1}/cdk and p13^{suc1}/cdk/Cyclin Complexes. We have previously reported that nucleotide analogues such as mant-ATP are powerful tools for monitoring the binding of cyclins to cdks (*29*). In this work, we have used the high sensitivity of mant fluorescence to quantify the interactions between cdks, cyclins, and p13^{suc1}. Our titration experiments reveal that monomeric p13^{suc1} can form stable complexes with monomeric cdk2 or cdc2 with relatively high affinity with a K_d of 150 and 180 nM, respectively, and clearly indicate that p13^{suc1} binding is not mediated via phosphorylation of residues Thr^{14} and Tyr^{15} in cdks.

The binding of monomeric p13^{suc1} to cdk2 induced a 2-fold increase in the fluorescence of mant-ATP, and as previously shown for cyclin A (*29*), the presence of p13^{suc1} reduced by a factor of 2 the release rate of mant-ATP displacement from cdk2. Our results indicate that the binding of p13^{suc1} to cdk2 modifies the conformation of the catalytic site or of the nucleotide binding site of cdk2 by closing the ATP binding pocket. According to the X-ray structure of the cdk2/CksHs1 complex, the binding of Cks proteins to cdk2 takes place in the C-terminal lobe of cdk2 but also induces a discrete change in the conformation of the N-lobe of cdk2, where residues 36−39 adopt a conformation similar to that of the activated cdk2/cyclin A complex (*38*, *42*, *43*). As the residues of CksHs1 at the interface with cdk2 are essentially conserved in p13^{suc1}, we can extrapolate this structure to p13^{suc1} and, based on our kinetic data, confirm that such a conformational change occurs in the catalytic domain of cdk2. However, binding of p13^{suc1} similarly reduced the dissociation rate of ATP and ADP from cdk2, in contrast to cyclin A, which was specific for the catalytic substrate ATP. From these data, we therefore conclude that the conformational change of cdks induced by the presence of p13^{suc1} may not be directly linked to the activation or inhibition of the catalytic mechanism of cdk2 but is more probably related to the regulation of cdks through binding of other proteins.

Overexpression of Cks proteins has been proposed to inhibit the cdc25-dependent dephosphorylation of cdc2 on residues Thr^{14} and Tyr^{15}. We have not observed a requirement for phosphorylation of these two residues for binding of p13^{suc1} to cdks. Moreover, from the X-ray structure of the CksH1/cdk2 complex it is clear that CksHs1 binds to the C-lobe of cdk2. Our data taken together with that of the structure of cdk2/CksHs1 suggest that Cks proteins do not directly prevent the dephosphorylation of cdk2 residues 14 and 15 by competing with cdc25 with respect to their binding site within the cdk, but rather through a conformational change in the cdks, for instance, in the ATP-binding pocket, thus modifying the orientation of residues Tyr^{14} and Thr^{15} with respect to their accessibility for cdc25.

The interface between cdk2 and CksHs1 is mainly form by α-helix 5 and L14 loop, and the sequence of these motifs is present only in cdk2, cdk3, and cdc2 but neither in cdk5 nor in cdk4, which accordingly do not interact with Cks proteins (*44*). Now we can extend this characteristic to cdk7, as no significant binding of p13^{suc1} to cdk7 or cdk7/cyclin H was observed. These data reveal a certain specificity in the interaction between p13^{suc1} and different cdks and cdk/cyclin complexes. In the case of cdk7, the lack of interaction is most likely due to differences in the structure of its C-lobe. Indeed, most of the side-chain residues in cdk2 which form the interface with CksHs1 are different in cdk7. In particular the residues forming the aromatic cluster at the interface between CksHs1 and cdk2 were shown to be essential, as a mutation in this domain in CDC28 (Pro250-Leu) completly abolished the binding of CksHs1 (*38*).

Of particular interest, the presence of cyclin associated to cdks did not affect binding of p13^{suc1} to cdks but instead seemed to increase the stability of the p13^{suc1}/cdk2/cyclin A

ternary complex by a factor of 2, with a dissociation constant between 70 and 90 nM for cdk2/cyclin A and cdc2/cyclin A, respectively. These results together with the lack of interaction between cyclin A and p13^{suc1} are in agreement with the model of two independent binding sites on cdk2 for cyclin A and Cks proteins (*38*). Indeed, according to the X-ray crystal structure of the cdk2/CksHs1 complex, CksHs1 binds exclusively to a continuous sequence of residues within α-helix 5 and L14 loop in the C-lobe of cdk2, far away from the cyclin binding domain on cdk2 (*42*, *43*). Moreover, the high stability of both binary cdk2/p13^{suc1} and ternary cyclin A/cdk2/p13^{suc1}complexes isolated by size exclusion chromatography in the presence of high salt concentrations confirms the mainly hydrophobic character of these interactions, as previously proposed from the X-ray data (*38*). The presence of a cyclin in a ternary p13^{suc1}/cdk2/cyclin complex may cooperate in strengthening the interaction between cdk and p13^{suc1}. Moreover the structural data reveal that binding of cyclin A to cdk2 may modify the orientation of the C-lobe of cdk2 (*42*, *43*), and we have argued that the binding of cyclin A to cdk2 exposes the hydrophobic patch of the L14 loop of cdk2 for the interaction with Cks proteins. This 2-fold increase in the affinity of p13^{suc1} for cdk2 in the presence fo cyclin A observed in vitro seems realistic and has recently been confirmed in *Xenopus* eggs, where it was shown that the presence of the cyclin stimulated binding of Cks proteins to cdks in vivo (*44*). The comparison of our results with the in vivo data from *Xenopus* extracts shows that a slight effect observed in vitro can in fact promote dramatic changes in a cellular context.

Transient kinetics demonstrated that binding of p13^{suc1} to cdk2 or the cdk2/cyclin A complex occurred in one single step, with k_{on} and k_{off} rate constants which were not significantly different from those proposed for binding of human CksHs1 using the Biacore system (*38*, *40*). These similarities tend to confirm that the human homologue of p13^{suc1} might complement depletion in yeast and vice versa and that the binding of CksHs1 or p13^{suc1} to cdk2 involves the same binding site (*9*). Interestingly, the presence of cyclin A did not modify the association rate of p13^{suc1} binding to cdk2 but decreased its off rate 3-fold, which suggests that the presence of cyclin A stabilizes the ternary complex. This high stability of the ternary complex and the conformational change induced by p13^{suc1} may reflect a restrictive event for the binding of substrate to cdk2/cyclin A or for the binding of cdc25 for the activation of cdk2. On the other hand, as the conformational change in cdk2 occurs close to the T-loop, binding of p13^{suc1} may restrict the access of the Cdk activating kinase (CAK), thus preventing phosphorylation of Thr^{160} and full activation of cdk2/cyclin A. Cks proteins contain a conserved positively charged cluster that has the potential to interact with phosphate or phosphorylated proteins. Moreover, it has recently been shown that p13^{suc1} could interact with the active phosphorylated form of the cyclosome. Taken together, these data have led to the hypothesis that the tight binding of Cks proteins to the cdk2/cyclin A complex might be a means of targeting it for degradation (*46*, *47*). That p13^{suc1} should present such an important affinity for cdk2 and cdk2/cyclin A indicates, as already suggested by other groups, that Cks proteins are likely to play a role in the regulation of the mutiple forms of cdk2 kinase throughout cell cycle progression (*14*, *48*).

Finally neither the strand-exchanged dimer nor the zinc-mediated dimeric form of p13^{suc1} interact with cdks or cdk/cyclin complexes. This result is not surprising, as the residues involved in dimer formation are directly involved in the interaction of the monomeric form of p13^{suc1} with cdk2 (*19*, *22*, *38*). Our results clearly show an effective competition between zinc and cdk2 for the same binding domain on p13^{suc1}, constistent with data from the X-ray structure of cksHs1/cdk2 and from the characterization of mutations of CksHs1 which have shown that the essential residues at the interface between cdk2 and CksHs1 are also involved in formation of strand-exchanged dimers (*38*, *40*). For instance, a mutation in the β-hinge domain (residues Tyr^{57}, Met^{58}, His^{60}, and Glu^{63}) favors strand-exchanged dimer formation but suppresses the binding of cks to cdk2. Moreover, a mutation in the β-strand 1 region (residues from Tyr^{12}, Glu^{15}, and Lys^{14}) forming the hydrophobic domain at the interface between CksHs1 and cdk2 also suppresses the binding of cks1 to cdk2 (*38*). Taken together, these results tend to suggest that dimerization may be a means of regulating excessive concentrations of p13^{suc1} in vivo. p13^{suc1} proteins may indeed adopt different conformations and assemble as multimers in reponse to changes in their environment during the cell cycle and thereby directly modulate the activity of cdk/cyclin complexes in vivo.

ACKNOWLEDGMENT

This work is dedicated to the memory of Dr. Jean-Claude Cavadore. We acknowledge Prof. M. Dorée for fruitful discussions and continuous support of this work. We also thank Dr. J. A. Endicott for providing the p13^{suc1} coordinates, Dr. D. Fesquet and Prof. S. Reed for helpful discussions, and Dr. F. Travers for suggestions concerning analysis of kinetics.

REFERENCES

1. Morgan, D. O. (1995) *Nature 374*, 131−134.
2. Morgan, D. O. (1996) *Curr. Opin. Cell Biol. 8*, 767−772.
3. Solomon, M. J. (1994) *Trend Biochem. Sci. 19*, 496−500.
4. Peter, M., and Herskowitz, I. (1994) *Cell 79*, 181−184.
5. Endicott, J. A., and Nurse, P. (1995) *Structure 3*, 321−325.
6. Hayles, J., Aves, S., and Nurse, P. (1986) *EMBO J. 5*, 3373−3379.
7. Hindley, J., Phear, G., Stein, M., and Beach, D. (1987) *Mol. Cell Biol. 7*, 504−511.
8. Moreno, S., Hayles, J., and Nurse, P. (1989) *Cell 58*, 361−372.
9. Richardson, H. E., Stueland, C. S., Thomas, J., Russell, P., and Reed, S. I. (1990) *Genes Dev. 4*, 1332−1344.
10. Pines, J. (1996) *Curr. Biol. 6*, 1399−1402.
11. Hayles, J., Beach, D., Durkarcz, B., and Nurse. *Mol. Gen. Genet. 202*, 291−293.
12. Hadwiger, J. A., Wittenberg, C., Mendenhall, M. D., and Reed, S. I. (1989) *Mol. Cell Biol. 9*, 2034−2041.
13. Brizuela, L., Draetta, G., and Beach, D. (1987) *EMBO J. 6*, 3507−3514.
14. Tang, Y., and Reed, S. I. (1993) *Genes Dev. 7*, 822−832.
15. Dunphy, W. G., Brizuela, L., Beach, D., and Newport, J. (1988) *Cell 54*, 423−431.
16. Patra, D., and Dunphy, W. G. (1996) *Genes Dev. 10*, 1503−1515.
17. Arion, D., Meijer, L., Brizuela, L., and Beach, D. (1988) *Cell 55*, 371−378.
18. Endicott, J. A., Noble, M. E., Garman, E. F., Brown, N., Rasmussen, B., Nurse, P., and Jhonson, L. N. (1995) *EMBO J. 14*, 1004−1014.

19. Bourne, Y., Arvai, A. S., Bernstein, S. L., Watson, M. H., Hickey, M. J., Reed, S. I., Endicott, J. A., Noble, M. E., Johnson, L. N., and Tainer, J. A. (1995) *Proc. Natl. Acad. Sci. U.S.A. 92*, 10232−10236.
20. Khazanovich, N., Bateman, K. S., Chernaia, M., Michalak, M., and James, M. N. G. (1996) *Structure 4*, 299−309.
21. Arvai, A. S., Bourne, Y., Hickey, M. J., and Tainer, J. A. (1995) *J. Mol. Biol. 249*, 835−842.
22. Parge, H. E., Arvai, A. S., Murtari, D. J., Reed, S. I., and Tainer, J. A. (1993) *Science 262*, 387−395.
23. Hiratsuka, T. (1983) *Biochim. Biophys. Acta 742*, 496−508.
24. John, J., Sohmen, R., Feuerstein, J., Linke, R., Wittinghofer, A., and Goody, R. S. (1990) *Biochemistry 29*, 6958−6965.
25. Labbé, J. C., Cavadore, J. C., and Dorée, M. (1991) *Methods Enzymol. 200*, 2291−2299.
26. Lorca, T., Labbé, J.-C., Devault, A., Fesquet, D., Capony, J.-P., Cavadore, J.-C., Le Bouffant, F., and Dorée, M. (1992) *EMBO J. 11*, 2381−2390.
27. Labbé, J. C., Martinez, A. M., Fesquet, D., Capony, J. P., Darbon, J. M., Derancourt, J., Devault, A., Morin, N., Cavadore, J. C., and Doree, M. (1994) *EMBO J. 13*, 5155−5164.
28. Devault, A., Martinez, A. M., Fesquet, D., Labbe, J. C., Morin, N., Tassan, J. P., Nigg, E. A., Cavadore, J. C., and Doree, M. (1995) *EMBO J. 14*, 5027−5036.
29. Heitz, F., Morris, M. C., Fesquet, D., Cavadore, J. C., Dorée, M., and Divita, G. (1997) *Biochemistry 36*, 4995−5003.
30. Bradford, N. M. (1976) *Anal. Biochem. 72*, 248−254.
31. Laemmli, U. K. (1970) *Nature 227*, 680−685.
32. Divita, G., Goody, R. S., Gautheron, D. C., and Di Pietro, A. (1993) *J. Biol. Chem. 268*, 13178−13186.
33. Calhoun, D. B., Vanderkooi, J. M., and Englander, S. W. (1983) *Biochemistry 22*, 1533−1539.
34. Eftink, M. R., and Ghiron, C. A. (1991) *Anal. Biochem. 114*, 199−227.
35. Wachsstock, D. H., and Pollard, T. D. (1994) *Biophys. J. 67*, 1260−1273.
36. Neyroz, P., Menna, C., Polverini, E., and Masotti, L. (1996) *J. Biol. Chem. 271*, 27249−27258.
37. Woody, R. W. (1994) *Eur. Biophys. J. 23*, 253−262.
38. Bourne, Y., Watson, M. H., Hickey, M. J., Holmes, W., Rocque, W., Reed, S. I., and Tainer, J. A. (1996) *Cell 84*, 863−874.
39. Reed, S. I., Hadwiger, J. A., and Lörincz, A. (1985) *Proc. Natl. Acad. Sci. U.S.A. 82*, 4055−4059.
40. Watson, M. H., Bourne, Y., Arvai, A. S., Hickey, M. J., Santiago, A., Bernstein, S. L., Tainer, J. A., and Reed, S. (1996) *J. Mol. Biol. 261*, 646−657.
41. Birck, C., Vachette, P., Welch, M., Swarén, P., and Samama, J.-P. (1996) *Biochemistry 35*, 5577−5585.
42. Jeffrey, P. D., Russo, A. A., Polyak, K., Gibbs, E., Hurwitz, J., Massagué, J., and Pavletich, N. P. (1995) *Nature 376*, 313−320.
43. Russo, A. A., Jeffrey, P. D., and Pavletich, N. P. (1996) *Nature Struct. Biol. 3*, 696−700.
44. Egan, E. A., and Solomon, M. J. (1998) *Mol. Cell. Biol. 18*, 3659−3667.
45. Azzi, L., Meijer, L., Ostvold, A.-C., Lew, J., and Wang, J. H. (1994) *J. Biol. Chem. 169*, 13279−13288.
46. Hershko, A. (1997) *Curr. Opin. Cell Biol. 9*, 788−799.
47. Sudakin, V., Shteinberg, M., Ganoth, D., Hershko, J., and Hershko, A. (1997) *J. Biol. Chem. 272*, 18051−18059.
48. Basi, G., and Draetta, G. (1995) *Mol. Cell. Biol. 15*, 2028−2036.

BI980913U